

A Nanoparticle Sampler Incorporating Differential Mobility Analyzers and Its Application at a Road-Side near Heavy Traffic in Kawasaki, Japan

Mariko Ono-Ogasawara¹, Toshihiko MYOJO^{2*}, Shinji Kobayashi³

¹ *National Institute of Occupational Safety and Health, Nagao, Tama, Kawasaki, 214-8585, Japan*

² *University of Occupational and Environmental Health, Iseigaoka 1-1, Yahata-nishiku, Kita-Kyushu, 807-8555, Japan*

³ *National Institute for Environmental Studies, Onogawa, Tsukuba, 305-8506, Japan*

Abstract

Diesel exhaust particles consist mainly of nanoparticles, the surfaces of which are covered with various organic chemicals such as polycyclic aromatic hydrocarbons (PAHs), some of which are known to be mutagenic or carcinogenic. Because some of these chemicals are volatile or semi-volatile, the fact that a differential mobility analyzer (DMA) operates at normal ambient pressure represents an advantage over many impactor-type samplers, which operate at half atmospheric pressure or less. In this study, we used twin custom-made DMAs as a nanoparticle sampler, and increased the sampling flow rate for each DMA separately. The sampler was used to sample ambient aerosol particulate matter (PM) at the side of a road carrying heavy traffic over a 4-day period. The average sizes of the aerosol particles collected were 80 and 240 nm. The PAHs on these particles were collected on quartz fiber filters and measured by direct-injection thermal-desorption gas chromatography/mass spectrometry. Twelve PAHs (3- to 6-ring PAHs), including benzo(a)pyrene, were analyzed quantitatively. The nanoparticles collected by the DMA sampler were richer in 5- to 6-ring PAHs than PM_{2.5} particles sampled in parallel. Scanning electron microscopy of the nanoparticles deposited on the DMA electrodes showed that the 240-nm particles (as classified by the DMA) were agglomerates of soot particles with a unit size of around 50nm or less, whereas the 80-nm particles consisted of single nanoparticles or agglomerates of a few particles.

Keywords: Differential mobility analyzer; Diesel exhaust particles; Nanoparticle; Carbon; Polycyclic aromatic hydrocarbons; Aerosol sampler.

*Corresponding author. Tel.: +81-93-691-7459;

Fax: +81-93-602-1782

E-mail address: tmyojo@med.uoeh-u.ac.jp

INTRODUCTION

Internal combustion engines, such as diesel

engines, generate exhaust nanoparticles containing various hydrocarbons. Following cooling in the vehicle's tail pipe and ambient air, these substances start to coagulate and/or condense into accumulation mode particles, which are of submicron size and used to be categorized as PM_{2.5} particles (Kittelson, 1998). PM_{2.5} particles are considered to be the main health hazard of air pollution (Dockery *et al.*, 1993). Diesel exhaust particles (DEP) are the main constituent of ambient aerosol particles, in particular at road-sides near heavy traffic. A combination of a differential mobility analyzer (DMA) and a condensation particle counter (CPC) is a useful tool for measuring the size distributions of DEP and the fine fraction of ambient particulate matter (PM). Using these instruments, many studies have measured the size distributions of road-side aerosols in urban areas, including our previous study carried out in a metropolitan area of Tokyo (Hasegawa *et al.*, 2004). The results showed a peak in the size range between 20 and 100 nm.

The origins of the carbon nanoparticles in PM has been estimated to be DEP (Shi *et al.*, 2001; Watson *et al.*, 2002; Sgro *et al.*, 2003; Vogt *et al.*, 2003; Philippin *et al.*, 2004). Aerosol particles were sampled using electrostatic precipitators or impactors. The particles were deposited onto grids or plates for subsequent analysis by transmission electron microscopy (TEM) or scanning electron microscopy (SEM). The morphology of PM and DEP as determined by TEM or SEM has been described (Ishiguro *et al.*, 1997; Wittmaack, 2002 and 2004). The aerosol

particles appeared mostly in agglomerates of nanoparticles with diameters of 30 nm.

Chemical analyses of the components have frequently been conducted to obtain information about the sources and hazards of ambient aerosols. Almost half of the particle mass of DEP consists of elemental carbon (EC). Their surfaces are covered with various kinds of organic carbon (OC) such as polycyclic aromatic hydrocarbons (PAHs), some of which are known to be mutagenic or carcinogenic. Size-selected samples obtained using low-pressure cascade impactors indicated different compositions for different sizes of particles (Venkataraman *et al.*, 1994).

When analyzing volatile and semi-volatile organic compounds, a DMA has an advantage over impactor-type nanoparticle-samplers in that it operates at normal ambient pressure, rather than at half atmospheric pressure or less. In this study, we used a custom-made nanoparticle sampler containing twin DMAs, and operated it at the side of a road carrying heavy traffic in Kawasaki, Japan. For the sampled PM, the sizes of which were 80 nm and 240 nm as classified by mobility diameter, we measured the PM mass, EC/OC mass, and quantitatively determined 12 PAHs. Also, the particles deposited on the electrodes of the DMAs were transferred to Nucleopore filters and observed by SEM.

METHOD

DMA Nanoparticle Sampler

The structure of the DMA has been published previously (Myojo *et al.*, 2002 and 2004). The

annular-type DMA has 5-cm and 3-cm outer and inner electrode diameters and the effective length is 40 cm. The DMA was operated at sheath flow rates of 6 L/min for laboratory sampling and 12 L/min for both laboratory and field sampling. It is easy to disassemble and assemble the DMA compared with other commercially available DMAs. The cleaning of electrodes to avoid cross-contamination should be required before sampling because DMA is a kind of electrostatic precipitator.

Fig. 1 shows the sampling train used for field measurements, which consisted of two DMA nanoparticle samplers and a PM_{2.5} sampler. The PM_{2.5} impactor in this train was the PM_{2.5} stage of a SIOUTAS impactor (Misra *et al.*, 2002) and was operated at 10 L/min (the designed flow rate of this impactor is 9 L/min). The sampling pumps were three sets of constant flow pumps (Σ -500, Sibata Scientific Co., Tokyo).

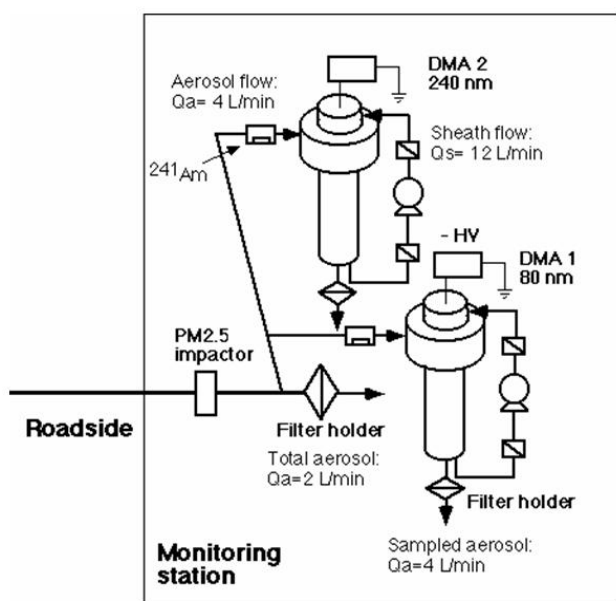


Fig. 1. The sampling train at the road-side at Ikegami-shincho.

Sampling Flow Rate of the DMA

The potential disadvantage of a DMA used as a sampler is its low sampling flow rate. We therefore adjusted the sampling flow rate of the DMA to increase the sample amounts. In general, the electrical mobility, Z_{pc} , of a particle extracted through the slit of an annular type DMA is as given by Knutsen and Whitby (1975):

$$Z_{pc} = \{Q_c + (1/2)(Q_a - Q_s)\} \ln(r_1/r_2) / (2\pi V L) \quad (1)$$

where Q_a : aerosol flow, Q_s : sample flow, Q_c : sheath flow, r_1/r_2 : electrode radius ratio, V : voltage on the electrode, L : electrode length.

The width of the mobility spread, Z_p , is calculated as:

$$\Delta Z_p = (Q_a + Q_s) \ln(r_1/r_2) / (2\pi V L) \quad (2)$$

The relationship between the electrical mobility, Z_p , and the particle diameter, d_p , is calculated as:

$$Z_p = p e C_m / (3\pi \mu d_p) \quad (3)$$

where p : number of charge, e : elementary charge, μ : viscosity, C_m : Cunningham's correction factor.

The relationship between the aerosol concentration, Δn_o , extracted through the DMA slit and the initial size distribution function of aerosol particles which have a positive (or negative) unit charge, N_i , of the size at Z_{pc} was determined by Kousaka *et al.* (1985) and is given below:

$$\Delta n_o = N_i \Delta Z p \quad (4)$$

Under common DMA operating conditions, $Q_a = Q_s$, thus:

$$\Delta n_o = N_i (2Q_a/Q_c) Z p c \quad (5)$$

As a result, the number of particles, N , collected on the filter per unit time is:

$$N = Q_a N_i (2Q_a/Q_c) Z p c \quad (6)$$

Eq. (6) means that if the aerosol flow rate, Q_a , is increased, the mass sampled is also increased. This, if Q_a is increased at the same sheath flow rate, the number of particles collected on the filter of the DMA outlet is proportional to the square of the sampling flow rate.

In order to increase aerosol concentration in sampling flow, the adjustment of flow rates at DMA has been tried by Tobias *et al.* (2001). As they used two real-time aerosol monitors, mainly sheath flow rate, Q_c , was reduced and Q_a/Q_c was 0.5. Eq. (6) showed that the increase of the aerosol flow rate, Q_a , is more effective as a nanoparticle sampler.

Charge Distribution of Ambient Aerosol Particles

Another potential disadvantage of a DMA used as a sampler is that particles must be charged to go through the DMA. We chose bipolar equilibrium charging by radioactive ion source, which is commonly used.

Sampled aerosol particles passed through an ^{241}Am ion source have an equilibrium charge

state known as the Boltzmann equilibrium (Takahashi, 1971; Liu and Pui, 1974). However, Boltzmann's law underestimates the charged fraction of nanoparticles, and thus Fuchs' theory (1963) should be used. As Fuchs' equations were complicated, we used empirical equations based on Fuchs' theory presented by Wiedensohler (1988). Calculated results for 50 to 240-nm particles are shown in Table 1. As we plan to compare the performance with low-pressure-type Andersen samplers (Tokyo Dylec Co. Tokyo), the sizes in the table were chosen based on the middle values for the 50% cut diameters (60, 120, 200 and 300 nm) of the last four stages of the sampler.

DMA extracts particles that have the same mobility. The charge distribution shown in Table 1 means that not only single-charged particles ($p = 1$) but also double- ($p = 2$) and triple- ($p = 3$) charged particles, which are larger than single-charged particles, are collected on the filter. SMPS or other measuring instruments using DMA eliminate the effects of multi-charged particles during the process of calculating the size distributions. However, the ratio of particles with double or larger charges needs to be considered for the application of the DMA nanoparticle sampler.

Performance Tests for the DMA

Before field application, we evaluated the performance of the DMA at a high sampling flow rate. The concentrations or size distribution of the aerosol particles classified by the DMA were measured by CPC (TSI model 3022) or Scanning Mobility Particle

Table 1. Selected electrical mobility of particle and their size and charge distributions.

Mobility	number of charge	p = +1	p = +2	p = +3
9.3E-4 (cm ² /Vs)	dp (nm)	50	73	92
Fuchs	R (-)	0.170	0.017	0.001
4.0E-4 (cm ² /Vs)	dp (nm)	80	120	154
Fuchs	R (-)	0.205	0.042	0.009
1.4E-4 (cm ² /Vs)	dp (nm)	150	235	314
Fuchs	R (-)	0.215	0.080	0.031
6.7E-5 (cm ² /Vs)	dp (nm)	240	397	546
Fuchs	R (-)	0.194	0.091	0.046

Sizer (SMPS; TSI model 3071 with model 3010) at our laboratory. The test aerosol used in this study was an ambient aerosol with additional incense smokes in a test chamber (25 m³). The test chamber, as shown in previous work (Ono-Ogasawara *et al.*, 2008a), supplied stable concentration of aerosol during tests.

Analysis of Carbon and PAHs

Quartz fiber filters (Whatman QMA, Whatman International Ltd., UK) were used to collect the particles at the DMA outlets. The filters had been heated at 400°C for 2 hours and weighed before sampling. The mass of aerosol particles was measured using a microbalance with a sensitivity of 10 µg; however, the amounts were insufficient (several were less than 10 µg) for measurement during field sampling. The mass of EC and OC on the filters was also determined using a carbon analyzer (Sunset Lab, OR, USA), based on NIOSH analytical method 5040 (Birch and Cary, 1996). DRI (Desert Research Institute) method (Chow *et al.*, 1993) is commonly used to measure EC and OC in ambient aerosol particles but our accessibility to the

instruments was main reason to choose the method. Uncertainty of measurement of the carbon analyzer is around 1 µg.

The PAHs on the particles collected on the quartz fiber filters were measured by a direct-injection gas chromatography/mass spectrometry (GC/MS) method (Ono-Ogasawara *et al.*, 2008a, b). Analysis was performed on a Porais Q Ion Trap GC/MS system (ThermoQuest, U.S.A), which consists of a FOCUS-DTD (Direct Thermal Desorption) system (GL Science, Japan). As a standard sample, SRM 1649a was used in this study. SRM 1649a is distributed by the National Institute of Standards and Technology (NIST, U.S.A) with certified analytical data for various chemical substances such as PAHs and polychlorinated biphenyls. Twelve PAHs (3- to 6-ring PAHs) including benzo(a)pyrene (BaP) were analyzed quantitatively within 25 minutes without any treatment. The detection limit of this method was less than 1 ng for each PAH.

Field Application

The DMA nanoparticle sampler shown in Fig. 1 was operated at the monitoring station near a road crossing in Ikegami-shincho,

Kawasaki, Japan. The main road passing through north east (to Tokyo) to south west (to Yokohama), which is 40 m wide and has double decks. The other road leading south east from the crossing is 25 m wide and connects to the industrial zone of Kawasaki. Around 60,000 vehicles use this road every day, 40% of which are heavy-duty trucks (Uehara et al., 2007). Several other monitoring instruments, including the SMPS (TSI model 3034), were also installed in the station, allowing us to obtain size distribution data for the ambient aerosols at the site.

The nanoparticle sampler was set to collect aerosol particles of 80 and 240 nm. Before field measurement, the DMA units, particularly the electrodes, were cleaned in a clean room and carefully reassembled. Sampling was conducted over 12 consecutive days in January-February 2005. It did not rain on any of the sampling days. The ambient temperature was ranging from 2 to 11°C. The filters were changed three times and the chemical analytical data presented in this study were for the first four days.

We observed particles deposited on the surfaces of electrodes. After 12 days sampling at the site, the DMAs were disassembled in a clean room. The particles deposited on the surfaces of the long, cylindrical electrodes could not be observed directly by SEM. Therefore, we cut small pieces of Nucleopore filter (pore size = 100 nm) and fixed them onto individual aluminum cells (10 mm in diameter and 5 mm in thickness) using conductive-carbon sticky-tape. We gently touched the filter paper pieces against the

electrode surface, rolling the cell a few times to ensure adequate transfer of the particles to the filter paper. A platinum coater was used to ion-coat the cell before SEM observation. A field emission type SEM (Hitachi S-4700) was used to observe the morphology of the particles deposited on the electrodes.

RESULTS AND DISCUSSION

Performance of DMA Nanoparticle Sampler

When sampling, the flow rate, Q_a , of the DMA was adjusted from 0.6 L/min to 2 L/min. Fig. 2 shows the size settings of the DMA and the particle concentration in the sampling flow measured by CPC (TSI model 3022). The particle concentration was increased almost 3-fold by increasing the flow rate, as predicted by Eq. (5); this means that the aerosol concentration increases proportionally to an increase in Q_a/Q_c .

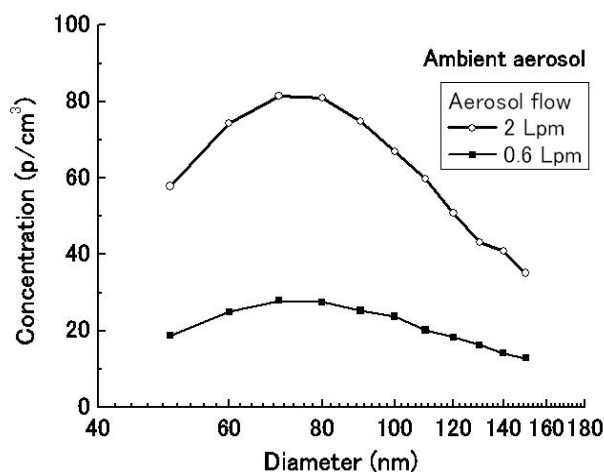


Fig. 2. The particle concentration of an ambient (indoor air) aerosol, measured at the DMA outlet using a condensation particle counter (TSI model 3022).

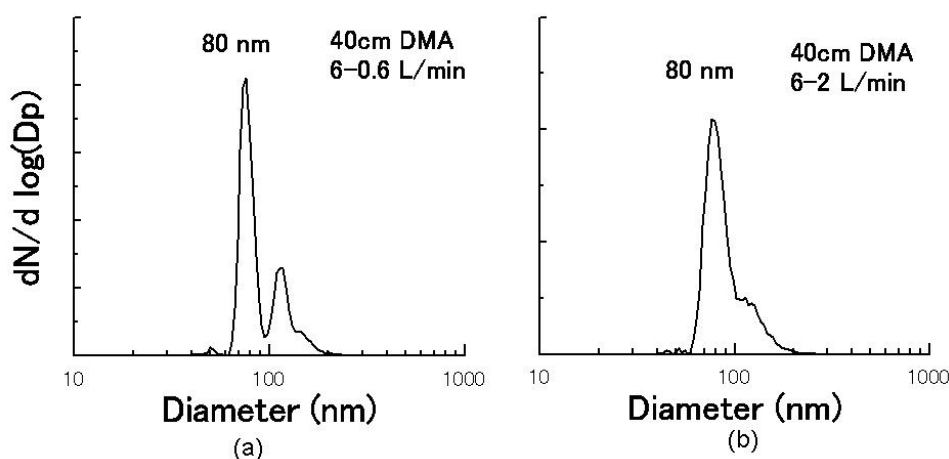


Fig. 3. The size distribution of a DMA outlet aerosol (incense smoke) measured by SMPS (TSI model 3071 with model 3010). The aerosol flow rate of the DMA was changed from 0.6 to 2 L/min.

The size distribution of the particles classified by the DMA was measured by SMPS (TSI model 3071 with model 3010) and the results are shown in Fig. 3. Fig. 3(a) shows the size distribution for 80nm particles at $Q_a/Q_c = 0.1$. If we set the DMA to perform steeper separation, we could not eliminate some of the double-charged particles. Fig. 3(b) shows the size distributions for 80nm particles at $Q_a/Q_c = 0.33$. When we increased Q_a/Q_c , the mobility spread, ΔZ_p , was expanded and the peaks for single- and double-charged particles overlapped. If we accept to sample both single- and double-charged particles using the DMA nanoparticle sampler, we can increase Q_a/Q_c to increase sampling mass, for example, $Q_a/Q_c = 0.5$ as Tobias *et al.* (2001).

As Eqs. (5) and (6) indicated that a higher aerosol flow rate will collect a larger mass of particles, we finally set the operating conditions for the DMA nanoparticle sampler to a sheath flow rate, Q_s , of 12 L/min and a sampling flow rate, Q_a , of 4 L/min. The performance of the DMA nanoparticle sampler

at the four size settings listed in Table 1 is shown in Fig. 4. The distributions of the particle sizes chosen for field operation, i.e. 80 and 240 nm, were separated from each other, as in Fig. 4. The optimum flow rate ratio, Q_a/Q_c , for the sampler will thus need to be confirmed in future studies.

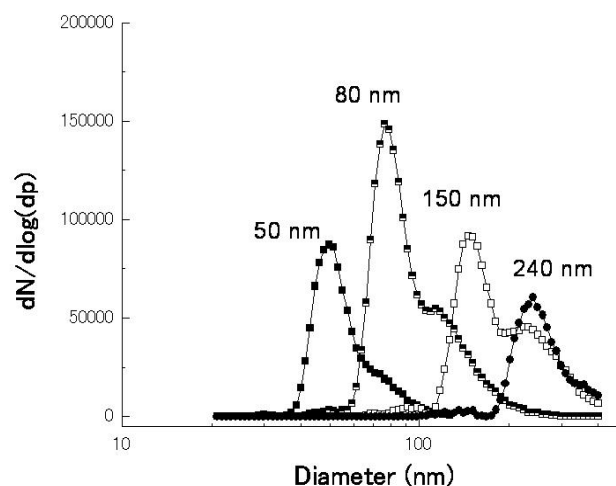


Fig. 4. The size distribution of a DMA outlet aerosol (incense smoke) measured by SMPS (TSI model 3071 with model 3010). The sheath flow rate was set at 12 L/min and the aerosol flow rate at 4 L/min.

Field Application

Aerosol Concentration

Table 2 summarizes the data for the particles sampled on the filters. The mass of particles collected on the filters of the DMA nanoparticle sampler was insufficient for measurement by a microbalance. However, it was sufficient for chemical analysis. Uncertainty regarding the mass measurement was caused partly by the absorption of water vapor and gaseous OC on the quartz fiber filters compared with Teflon filters. Therefore, a high-performance microbalance (with a sensitivity of less than 1 µg) may not solve the problem. The results from the carbon analyzer showed that the 240-nm particles consisted of EC and OC whereas the 80-nm particles consisted mainly of OC. The sampled nanoparticles were richer in 5- to 6-ring PAHs than PM_{2.5}; this is illustrated by the data for BaP, a typical substance found in DEP.

We then calculated the mass of the particles using SMPS data and the values in Table 1, as shown in Table 3. The table shows the calculation process for each number of charged particles. The calculated mass, M, on the filter of the sampler can be expressed as:

$$M_{p=1 \text{ to } 3} = (\pi dp^3/6) (R_{p=1 \text{ to } 3}) (\rho_{\text{effect}}) (n_i v \text{ dlogdp}) \quad (7)$$

where dp is the diameter of the particles (assumed to be spherical), R_{p=1 to 3} is the charge distribution of the particles which have p charge(s) (see Table 1), ρ_{effect} is the effective density, n_i is the size distribution function of particles within the size ranges (peak diameters

are 83 nm and 245 nm) measured by SMPS, v is the sampling air volume as shown in Table 3. The size range, dlogdp, was 0.35 for all sizes during these measurements and was calculated as follows:

$$d\log dp = 0.5 \log(dp_{Z_p-\Delta Z_p} / dp_{Z_p+\Delta Z_p}) \quad (8)$$

where dp_{Z_p-ΔZ_p} and dp_{Z_p+ΔZ_p} are the corresponding diameters at the mobilities Z_p-ΔZ_p and Z_p+ΔZ_p. We summed the mass values for single- to triple-charged particles (p = 1 to 3) as shown in Table 3. The 240-nm particles included 5% triple-charged particles, as shown in Table 1, but these triple-charged particles (around 550 nm particles) were not observed by SMPS. The estimated mass (25 µg) of 80-nm particles was similar to the measured mass (30 µg) for ρ_{effect} = 1 g/cm³. The difference between the estimated mass (92 µg) and the measured mass (50 µg) for 240-nm particles was considerable for ρ_{effect} = 1 g/cm³.

McMurry *et al.* (2002) measured the relationship between electrical mobility and mass for nano-size to submicron-size particles in urban atmospheric aerosols. Observed values for effective densities of these aerosol particles were classified into less massive particles (0.25-0.64 g/cm³) and more massive particles (1.7-2.2 g/cm³). They suggested that the less massive particles consisted of chain-agglomerate soot. Densities and fractal dimensions have also been studied by other groups (Maricq *et al.*, 2000; Olfert *et al.*, 2007; Symonds *et al.*, 2007).

Park *et al.* (2003) measured DEP mass and reported that the effective density of 50-nm

Table 2. Measured data at heavy traffic road side.

	PM _{2.5}	80 nm DMA	240 nm DMA
Sampling volume, V (m ³)	11.2	22.4	21.8
Collected particle mass* (μg)	600	30	50
OC (μg)	195	23.5	28.9
EC (μg)	172	5.4	12.0
Total PAH (ng)	239	22.9	51.8
BaP (ng)	12.9	1.5	3.8

*Sensitivity of the microbalance used in this study was 10 μg

Table 3. Measurement results at 2005/1/24–28, Ikegemi-shincho, Kawasaki.

DMA	d log dp: 0.35					
	80 nm DMA			240 nm DMA		
p: number of charge	p = +1	p = +2	p = +3	p = +1	p = +2	p = +3
dp (nm)	80	120	154	240	397	546
n _i (average for the days)	38100	26000	16200	6030	1190	NA
R (-)	0.205	0.042	0.009	0.194	0.09	0.046
effective density (g/cm ³)	1	1	1	1	1	
mass(μg)	16	7	2	64	27	NA
estimated mass from size distribution data (g)			25			92
effective density (g/cm ³)*	0.84	0.67	0.55	0.36	0.3**	NA
mass(μg)	13	5	1	23	8	
estimated mass from size distribution data (μg)			19			31
Measurement results 2005/1/24-28						
Mass on the filter (g)			30			50
Total carbon on the filter (μg)			28.9			40.9
Calculated ideal sampling of target particles						
Total mass of p = 1	p = 1	p = 1		p = 1	p = 1	
dp (nm)	80	80		240	240	
n _i (average for the days)	38100	38100		6030	6030	
R (-)	1	1		1	1	
effective density (μg/cm ³)	1	0.84		1	0.36	
estimated mass(μg)	78	65		333	120	

*interpolated from data by Park *et al.* (2003)

**estimated from data by Park *et al.* (2003)

particles sampled by DMA was almost 1 g/cm^3 but the density of 240-nm particles was half that of 80-nm particles. They observed chain-agglomerates of DEP which had low density. As shown in Table 3, we also estimated particle density based on the data by Park *et al.* (2003) and recalculated the particle mass. Recalculated mass was $19 \text{ }\mu\text{g}$ of 80-nm particles and $31 \text{ }\mu\text{g}$ of 240-nm particles. Our results showed good agreement with the measured mass and the total amount of carbon. This suggests that the ambient particles sampled at the roadside near heavy traffic contain carbon-rich agglomerates.

The DMA nanoparticle sampler collects only charged particles on the filter, and the ratio of charged particles shown in Table 3 is less than unity. In order to estimate the collection performance of the sampler, we calculated the total mass on the target size, shown in last line of Table 3. Although around one third of the mass of particles in sampled aerosol are collected by the DMA sampler, we

can estimate the mass collected on the filter of the DMA sampler theoretically and experimentally.

Particle Morphology

Fig. 5 shows the particles deposited on the electrode of the 80-nm DMA. The location on the electrode (10, 20 or 38 cm from the aerosol inlet, with a tolerance of $\pm 1 \text{ cm}$) corresponds to the classified size of particles shown in the figure. As we expanded ΔZ_p , the location on the electrode was not shown to be highly size-selective; however, nanoparticles could easily be observed without any interference by larger particles.

In ambient particles sampled at the road-side, we found non-volatile nanoparticles consisted of a single particle or agglomerates of a few particles. These nanoparticles were presumably consisting of elemental carbon. Although the mass of OC (which includes volatile species, such as those found in secondarily formed nanoparticles) was larger than the mass of EC, as shown in Table 3, we

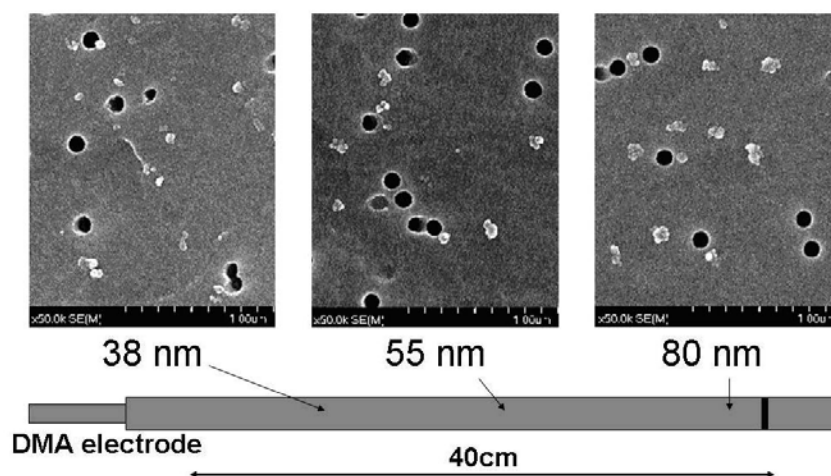


Fig. 5. Ambient particles deposited at three points on the 80-nm DMA electrode surface (transferred to a Nucleopore filter with a pore size of 100 nm).

could not observe these OC particles in SEM photos because they evaporated from the particles or totally disappeared under the high-vacuum conditions required for electron microscopy.

Fig. 6 shows the particles deposited on the electrode of the 240-nm particle DMA. SEM observation of the deposited particles also indicated that the 240-nm particles classified by DMA were agglomerates of around 50 nm-particles. These agglomerates were commonly observed in diesel soot particles and had a lower density than compact particles. The different deposition sites collected differently sized particles or agglomerates. The sizes and shapes of these particles were similar to those of the DEP reported by Park *et al.* (2003).

PAHs in Sampled PM

The profiles of the PAHs in roadside PM sampled by the 80-nm DMA, the 240-nm DMA and the PM_{2.5} detector are shown in Fig. 7 (a-c). Each DMA sample shows a different

profile and the PM collected by the DMA samplers is richer in 5- to 6-ring PAHs than the PM_{2.5} sample. Chrysene (CHR) is observed in the highest concentration among the PAHs in PM sampled by the DMA nanosamplers, whereas pyrene (PYR) levels are highest in PM_{2.5}. The total level of PAHs in the samples classified by the DMA sampler is almost one-tenth of that found in PM_{2.5}, but the total mass of, and amounts of PAH in, the original particle sample was estimated to be around 3 times higher than the values shown here, as discussed above.

Total and individual PAH concentrations measured at the site were similar to the values for PAHs in the particulate phase found during roadside monitoring by Harrison *et al.* (1996); Schauer *et al.* (2003); Ciganek *et al.* (2004) and many other studies. In this paper, we have focused on the performance of the DMA nanoparticle sampler. A detailed discussion regarding the chemical analysis of the collected particles will be presented separately.

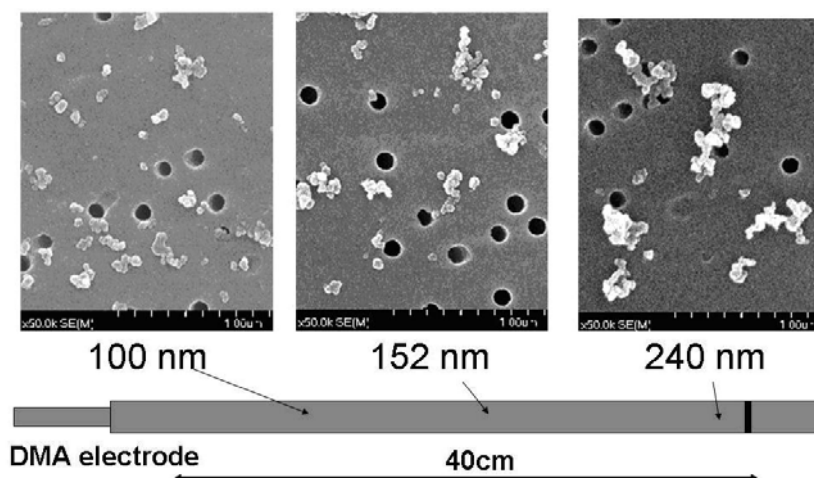


Fig. 6. Ambient particles deposited at three points on the 240-nm DMA electrode surface (transferred to a Nucleopore filter with a pore size of 100 nm).

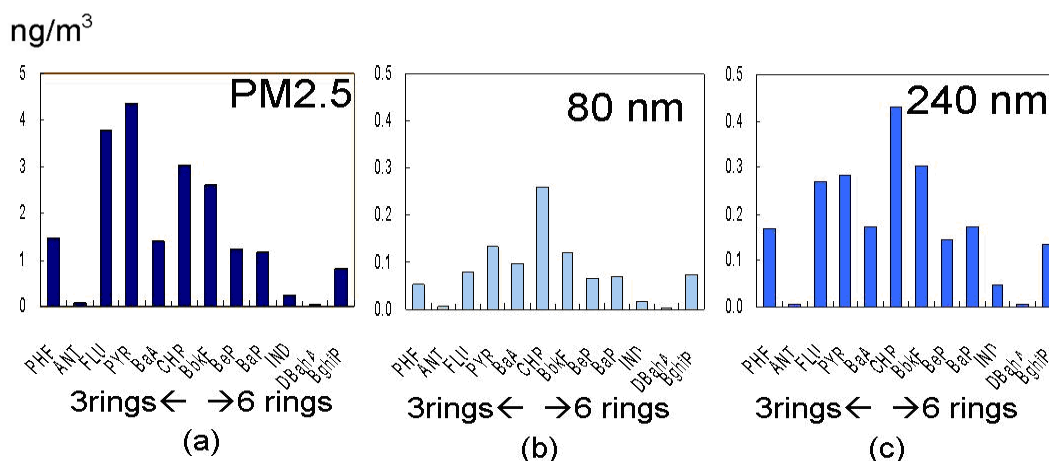


Fig. 7. PAH concentrations in samples collected at Ikegami-shincho.

CONCLUSIONS

DMAAs can be successfully used as nanoparticle samplers similar to impactors when the flow ratio (Q_a/Q_c) is increased. The DMA nanoparticle sampler will collect nanoparticles following charge distribution theory shown in this study. Additionally, size-selected nanoparticles collected on the DMA electrodes can be observed using SEM.

A few tens of micrograms of particulates were collected on the filters at the side of a busy road over four days. This was not enough to allow gravimetric methods to be used to determine the mass concentration, but was sufficient to allow chemical analysis such as carbon analysis and PAH identification using GC/MS.

ACKNOWLEDGEMENTS

The authors would like to thank Hidetsuru Matsushita, Professor Emeritus of the University of Shizuoka, for his important suggestions regarding atmospheric aerosol

monitoring. We would also like to express our gratitude to the members of the Kawasaki Municipal Research Institute for Environmental Protection and the Green Blue Corporation for their assistance with the roadside sampling. This work was partly supported by JSPS KAKENHI 20590621.

REFERENCES

- Birch, M.E. and Cary, R.A. (1996). Elemental Carbon-based Method for Monitoring Occupational Exposures to Particulate Diesel Exhaust. *Aerosol Sci. Technol.* 25: 221-224.
- Chow, J.C., Watson, J.G., Pritchett, L.C., Pierson, W.R., Frazier, C.A. and Purcell, R.G. (1993). The DRI Thermal/optical Reflectance Carbon Analysis System: Description, Evaluation and Applications in U.S. Air Quality Studies. *Atmos. Environ.* 27: 1185-201.
- Ciganek, M., Neca, J., Adamec, V., Janosek, J. and Machala, M. (2004). A Combined Chemical and Bioassay Analysis of Traffic

- Emitted Polycyclic Aromatic Hydrocarbons. *Sci. Total Environ.* 334-335: 141-148
- Dockery, D.W., Pope, C.A. III, Xu, X.P., Spengler, D.J., Ware, H.J., Fay, E.M., Ferris, G.B. and Speizer, E.F. (1993). An Association between Air Pollution and Mortality in Six U.S. Cities. *New Engl. J. Med.* 329: 1753-1759.
- Fuchs, N.A. (1963). On the Stationary Charge Distribution on Aerosol Particles in a Bipolar Ionic Atmosphere. *Pure Appl. Geophys.* 56: 185-193.
- Harrison, R.M., Smith, D.J.T. and Luhana, L. (1996). Source Apportionment of Atmospheric Polycyclic Aromatic Hydrocarbons Collected from an Urban Location in Birmingham, U.K. *Environ. Sci. Technol.* 30: 825-832.
- Hasegawa, S., Hirabayashi, M., Kobayashi, S., Moriguchi, Y., Kondo, Y., Tanabe, K. and Wakamatsu, S. (2004). Size Distribution and Characterization of Ultrafine Particles in Roadside Atmosphere. *J. Environ. Sci. Health., Part A.* 39: 2671-2690.
- Ishiguro, T., Takatori, Y. and Akihama, K., (1997). Structure of Diesel Soot Particles Probed by Electron Microscopy: First Observation of Inner Core and Outer Shell. *Combust. Flame.* 108: 231-234.
- Kittelson, D.B., (1998). Engines and Nanoparticles: A review. *J. Aerosol Sci.* 29: 575-588.
- Knutson, E.O. and Whitby, K.T. (1975). Aerosol Classification by Electric Mobility: Apparatus, Theory and Application. *J. Aerosol Sci.* 6: 443-451.
- Kousaka, Y., Okuyama, K. and Adachi, M., (1985). Determination of Particle Size Distribution of Ultra-fine Aerosols Using a Differential Mobility Analyzer. *Aerosol Sci. Technol.* 4: 209-225.
- Liu, B.Y.H. and Pui, D.Y.H. (1974). Equilibrium Bipolar Charge Distribution of Aerosols. *J. Colloid Interface Sci.* 49: 305-312.
- Maricq, M.M., Podsiadlik, D.H. and Chase, R.E. (2000). Size Distributions of Motor Vehicle Exhaust PM: A Comparison between ELPI and SMPS Measurements. *Aerosol Sci. Technol.* 33: 239-260.
- McMurry, P.H., Wang, X., Park, K. and Ehara, K. (2002). The Relationship between Mass and Mobility for Atmospheric Particles: A New Technique for Measuring Particle Density. *Aerosol Sci. Technol.* 36: 227-238.
- Myojo, T., Takaya, M. and Ono-Ogasawara, M. (2002). DMA as a Gas Converter from Aerosol to "Argosol" for Real-Time Chemical Analysis Using ICP-MS. *Aerosol Sci. Technol.* 36: 76-83.
- Myojo, T., Ehara, K., Koyama, H. and Okuyama, K. (2004). Size Measurement of Polystyrene Latex Particles Larger than 1 Micrometer Using a Long Differential Mobility Analyzer. *Aerosol Sci. Technol.* 38: 1178-1184.
- Olfert, J.S., Symonds, J.P.R. and Collings, N.J. (2007). The Effective Density and Fractal Dimension of Particles Emitted from a Light-duty Diesel Vehicle with a Diesel Oxidation Catalyst. *J. Aerosol Sci.* 38: 69-82.
- Ono-Ogasawara, M., Myojo, T., Kagi, N., Nishimura, N. and Fujii, S. (2008a). Quick

- Determination of Nicotine and PAHs in Fine Particulate Matter in Environmental Tobacco Smoke by Direct Injection-Thermal Desorption-GC/MS. *Earozoru Kenkyu*. 23: 200-209. (in Japanese).
- Ono-Ogasawara, M., Myojo, T. and Smith T.J. (2008b). A Simple Direct Injection Method for GC/MS Analysis of PAHs in Particulate Matter. *Ind. Health*. 46: 582-593.
- Park, K., Cao, F., Kittelson, D.B. and McMurry, P.H. (2003). Relationship between Particle Mass and Mobility for Diesel Exhaust Particles. *Environ. Sci. Technol*. 37: 577-583.
- Philippin, S., Wiedensohler, A. and Stratmann, F. (2004). Measurements of Non-volatile Fractions of Pollution Aerosols with an Eight-Tube Volatility Tandem Differential Mobility Analyzer (VTDMA-8), *J. Aerosol Sci*. 35: 185-203.
- Schauer, C., Niessner, R. and Pöschl, U. (2003). Polycyclic Aromatic Hydrocarbons in Urban Air Particulate Matter: Decadal and Seasonal Trends, Chemical Degradation, and Sampling Artifacts. *Environ. Sci. Technol*. 37: 2861-2868.
- Shi, J.P., Evans, D.E., Khan, A.A. and Harrison, R.M. (2001). Source and Concentration of Nanoparticles (< 10 nm Diameter) in the Urban Atmosphere. *Atmos. Environ*. 35: 1193-1202.
- Sgro, L.A., Basile, G., Barone, A.C., D'Anna, A., Minutolo, P., Borghese, A. and D'Alesio, A. (2003). A Detection of Combustion Formed Nanoparticles. *Chemosphere*. 51: 1079-1090.
- Symonds, J.P.R., Reavella, K.S.J., Olfert, J.S. Campbell, B.W. and Swift, S.J. (2007). Diesel Soot Mass Calculation in Real-time with a Differential Mobility Spectrometer. *J. Aerosol Sci*. 38: 52-68.
- Takahashi, K. (1971). Numerical Verification of Boltzmann's Distribution for Electrical Charge of Aerosol Particles. *J. Colloid Interface Sci*. 35: 508-510.
- Tobias, H.J., Beving, D.E., Ziemann, P.J., Sakurai, H., Zuk, M., McMurry P.H., Zarling, D., Waytulonis, R. and Kittelson, D.B. (2001). Chemical Analysis of Diesel Engine Nanoparticles Using a Nano-DMA/thermal Desorption Particle Beam Mass Spectrometer. *Environ. Sci. Technol*. 35: 2233-2243.
- Uehara, K., Hayashi, S., Yamao, Y., Matsumoto, Y. and Wakamatsu, S. (2007). Air Pollution at a Busy Urban Crossroad: Estimation of Annual Mean NO_x Concentration Distribution from Field Observations and Wind-tunnel Experiments. *J. of Japan Soc. for Atmos. Environ*. 42: 93-106.
- Venkataraman, C., Lyons, J.M. and Friedlander, S.K. (1994). Size Distributions of Polycyclic Aromatic Hydrocarbons and Elemental Carbon. 1. Sampling, Measurement Methods, and Source Characterization. *Environ. Sci. Technol*. 28: 555-562.
- Vogt, R., Kirchner, U., Scheer, V., Hinz, K.P., Trimborn, A. and Spengler, B. (2003). Identification of Diesel Exhaust Particles at an Autobahn, Urban and Rural Location Using Single-Particle Mass Spectrometry, *J. Aerosol Sci*. 34: 319-337.
- Watson, J.G., Chow, J.C., Lowenthal, D.H.,

- Stolzenberg, M.R., Kreisberg, N.M. and Hering, S.V. (2002). Particle Size Relationship at the Fresno Supersite. *J. Air Waste Manage. Assoc.* 52: 822-827.
- Widensohler, A. (1988). An Approximation of the Bipolar Charge Distribution for Particles in the Submicron Size Range. *J. Aerosol Sci.* 19: 387-389.
- Wittmaack, K. (2004). Characterization of Carbon Nanoparticles in Ambient Aerosols by Scanning Electron Microscopy and Model Calculations. *J. Air Waste Manage. Assoc.* 54: 1091-98.
- Wittmaack, K. (2002). Impact and Growth Phenomena Observed with Sub-micrometer Atmospheric Aerosol Particles Collected on Polished Silicon at Low Coverage. *Atmos. Environ.* 36: 3963-3971.

Received for review, October 13, 2008

Accepted, January 22, 2009